Mass Transfer and Friction Factor in Adiabatic Annular Air–Water Flow

Šefko Šikalo and Wael Avdović
Faculty of Mechanical Engineering
University of Sarajevo
Sarajevo, Bosnia and Herzegovina
sikalo@mef.unsa.ba

***Abstract*—In this study, an annular water–air flow under adiabatic conditions is investigated. Mass transfer by the evaporation from a wall liquid film into the air flowing inside a tube is studied. A series of experiments were performed, in order to investigate effects of the water flow rate, the air flow rate and the air humidity on water evaporation and the pressure drop in the annular flow. The experimental results are presented and correlated in terms of dimensionless numbers, namely Sherwood, Reynolds and Schmidt number.**

Keywords— annular two-phase flow, liquid film, mass transfer coefficient, friction factor

I. INTRODUCTION

Problems involving heat and mass transfer in two-phase flows arise in power plants, cryogenics, chemical engineering and food processing. Methods based on analogy between heat, mass and momentum transfer in single-phase flows are commonly used to explain the mechanism of heat and mass transfer in two-phase flows. From the literature review it is clear that there are no direct experimental evidence about the analogy between heat, mass and momentum transfer in two-phase flows.

The measurements regarding the two-phase flows are rather complicated and new data are necessary to obtain a better insight into the evaporation from a liquid film. The heat or mass transfer from a liquid film is fundamentally influenced by the presence of free surface waves [1,2,3,4]. However, the exact theory describing the mechanism of the transport enhancement particularly for a liquid film flows with irregular interfacial structures, is still not fully established. Most mass transport measurements on liquid films are conducted in wetted wall columns. The mass transfer rate was investigated by numerous researchers. However, the influence of the liquid flow rate on the rate of evaporation has not been investigated yet [5].

An overview of early relevant works in this field is provided by [6], further references can be found in the work of [7]. The rate of gas-side mass transfer of liquid films on strongly curved surfaces has not been investigated yet. The liquid-side mass transfer of planar films has also been investigated by a number of authors [8, 9,10,11].

In all the experiments mentioned above, the gas flow rate was relatively low and an interaction of liquid and gas-phase fluid dynamics was not considered. Mass transfer experiments at high Reynolds numbers of gas and liquid were carried out by [12] in a wetted wall column in concurrent flow.

Friction factor is a very important parameter to characterize the pressure drop in a two-phase flow. An excellent review and collection of references, which refer to the friction factor in two-phase flows, could be fined in [13].

In this work we experimentally investigate the adiabatic evaporation and the pressure drop in the annular two-phase flow with very low water flow rate and observed the pressure reduction.

II. ANALYTICAL CONSIDERATIONS

A. Adiabatic evaporation of annular liquid film

In order to understand the annular flow and its influence on the mass transfer coefficient, the physical parameters that are relevant to the problem are considered in this study.

Mass transfer of the water (*A*) evaporation into the air (*B*) inside the wetted-wall tube first has been considered analytically. Liquid water film flows on the inner wall of the tube while the air flows through the core of the tube (annular flow) as illustrated in Fig. 1. Dry air enters the bottom of the wetted section at ambient temperature and atmospheric pressure.

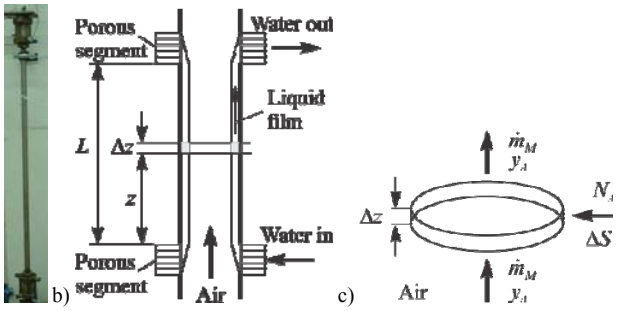

Fig. 1. Wetted-wall section: (a) a photograph of the test section, (b) schematic diagram and (c) differential element of the section.

The water can enter the top or the bottom of the test section, depending on the air speed forming a co-current or a counter-

current flow. The water evaporates from the air-water interface due to the difference between the partial pressure of saturation and the vapor partial pressure, $p_A^* - p_A(z)$ as a driving force. Partial vapor pressure in the air stream increases from $p_A(z) = p_{A\text{in}}$ at the inlet of the test section, to $p_A(y) = p_{A\text{out}}$ at the outlet of the test section. It is reasonable to assume that the initial value of the overall gas flow remains almost constant and that the gas behavior is of the dry air. The temperature and the pressure are assumed constant as well. Therefore, Reynolds and Schmidt numbers of the air are constant along the section and, consequently, the mass transfer coefficient is constant [14]. The water balance (component *A*) for a differential element of the wetted tube Δz, at a steady-state evaporation and a constant molar gas flux, $\dot{m}_M = c\bar{u}$, is expressed as

$$\frac{D^2\pi}{4}\dot{m}_M y_A\big|_{z+\Delta z} - \frac{D^2\pi}{4}\dot{m}_M y_A\big|_z = \frac{D^2\pi}{4}\Delta z a N_A \tag{1}$$

where y_A is mole fraction of the water vapor inside the gas phase, *S* is the evaporation area and *D* is the section diameter. By substituting $a = \Delta S/\Delta V$, Eq. (1) can be written as

$$\frac{D^2\pi}{4}\dot{m}_M y_A\big|_{z+\Delta z} - \frac{D^2\pi}{4}\dot{m}_M y_A\big|_z = \frac{D^2\pi}{4}\Delta z a N_A \tag{2}$$

Applying the boundary conditions as $\Delta z \to 0$, we have

$$\dot{m}_M \frac{dy_A}{dz} = aN_A = k_G a\left(p_A^* - p_A\right) \tag{3}$$

where p_A^* is the vapor pressure and $y_A = p_A/p$. Finally, the mass transfer coefficient can be written as

$$k_G = \frac{\dot{m}_M D}{4pL}\ln\left[\frac{p_A^* - p_{A\text{in}}}{p_A^* - p_{A\text{out}}}\right] \tag{4}$$

where *L* is the overall height of the wetted section. For diluted solutions one may assume $\mathrm{Sh} = k_G RTD/D_{AB}$, where *R* is the molar gas constant. The Sherwood number is

$$\mathrm{Sh} = \frac{D}{4L}\mathrm{ReSc}\cdot\ln\left[\frac{p_A^* - p_{A\text{in}}}{p_A^* - p_{A\text{out}}}\right] \tag{5}$$

Thus, $\mathrm{Sh} = f(\mathrm{Re},\mathrm{Sc})$. The mass flux of the gas phase is $\dot{m} = \rho u_\mathrm{G}$, its molar flux is $\dot{m}_M = \dot{m}/M$, the Reynolds number is $\mathrm{Re} = \dot{m}D/\mu$, and $\mathrm{Sc} = \nu/D_{AB}$. The air properties (ρ, μ, D_{AB} i Sc) depend on the temperature and the pressure. The vapor concentration in the air flow is $c_{A\text{out}} = p_{A\text{out}}/RT$, which is determined from the air humidity at the inlet and the outlet of the test section. The mass transfer coefficient and Sh number was determined using Eq. (4), and Eq. (5), respectively.

B. Friction factor in an annular flow

The interfacial stress, τ_i, represents the drag on the liquid film. It is desired to predict the dependence of τ_i on the flows of the gas and of the liquid film. The solution of this problem is central to predicting the behavior of gas–liquid flows. The interfacial stress is determined by measuring the gas-phase pressure gradient and the height of the liquid layer under conditions of a fully developed symmetric flow. The interfacial stress is usually described in terms of a friction factor, f_i, so that

$$\tau_\mathrm{i} = \frac{f_\mathrm{i}}{2}\rho_G u_\mathrm{G}^2 \tag{6}$$

where u_G is gas velocity. If the interface is smooth, f_i is the same as is found for flow over smooth solid surfaces, designated as f_S. However, the presence of waves at the interface can lead to very large values of $f_\mathrm{i}/f_\mathrm{S}$, which are related to the amplitudes of the waves.

For a smooth surface with a single-phase turbulent flow, the friction factor can be approximated by [15],

$$f_\mathrm{S} = 0.046\,\mathrm{Re}_\mathrm{G}^{-0.2} \tag{7}$$

where Re_G is the gas-phase Reynolds number.

The liquid film Reynolds number is defined as

$$\mathrm{Re}_\mathrm{LF} = \frac{4M_\mathrm{LF}}{D\pi\mu_\mathrm{L}} \tag{8}$$

where M_LF is the liquid film mass flow rate. The Colburn–Carpenter hypothesis gives dimensionless height of the liquid layer around the circumference [16],

$$\delta_\mathrm{G}^+ = \left[(0.707\,\mathrm{Re}_\mathrm{LF}^{0.5})^{2.5} + (0.0379\,\mathrm{Re}_\mathrm{LF}^{0.9})^{2.5}\right]^{0.4} \tag{9}$$

Thus, Eq. (9) provides the value of $\delta^+ = \delta u^*/\nu$ for a given flow rate of the film. Therefore, average height of the liquid layer around the circumference could be estimated,

$$\delta_\mathrm{G} = \delta_\mathrm{G}^+\nu_\mathrm{G}/u_\mathrm{G}^* \tag{10}$$

Asali *et al*. [17] measured interfacial stress for upward vertical annular flows and chose a scaling based on the viscous length for the gas phase. Particular attention was given to low liquid rates and high gas velocities for which the film can have thicknesses of 30 to 200 μm. The following relation for the friction factor was obtained at $u_\mathrm{G} > 25$ m/s

$$\frac{f_\mathrm{i}}{f_\mathrm{S}} - 1 = 0.45(\delta_\mathrm{G}^+ - 4) \tag{11}$$

where $\delta_\mathrm{G}^+ = \delta u_\mathrm{G}^*/\nu_\mathrm{G}$ is the ratio of the film height to a gas-phase length scale, ν_G is kinematic viscosity of the gas and $u_\mathrm{G}^* = (\tau_\mathrm{i}/\rho_\mathrm{G})^{1/2}$ is the friction velocity, using the shear stress at interface. Approximations for δ_G^+ both in the ripple and disturbance wave regimes are suggested by [17].

III. EXPERIMENTAL SET-UP AND MEASUREMENT TECHNIQUES

A schematic of the experimental apparatus is shown in Fig. 2. Both adiabatic evaporation and pressure drop experiments

were carried out on the apparatus. It is the same as that described by [18].

Two vertical test sections are used. A Plexiglas test section, smooth tube with the average roughness R_a=0.01 μm, 14 mm inner diameter (ID) and 980 mm (L/D=70) long, and a stainless steel (SS 304) technically smooth tube with R_a=3.37 μm, 13.2 mm ID and 924 mm (L/D=70) long. A flow development section of 60 tube diameter (L_e/D=60) is used to ensure that turbulent air flow is fully developed at the test section inlet. Porous segment connected to gas–liquid separators are used to inject the liquid into the test section to form the liquid wall film and to remove the liquid wall film at the other side of the test section. The porous segments are constructed from stainless steel washers of the same internal diameter as he test section and 45 mm long. The distance between two washers is 0.1 mm. The washer assembly is enclosed in a Plexiglas cylinder shutter, and is provided with a drain that is connected to a pump (second porous section to inject water) while other two porous sections are connected to the cyclone gas–liquid separators (11a,b). The test section pressure forced the liquid out of the pipe trough the porous section into the cyclone gas–liquid separators and water are collected into a measuring vessel. Some gas is inevitable removed with the liquid and it is important to minimize its rate. In the measurement described here the gas take-off at an porous segment was typically around 0.5% of the total gas flow through the test section, and is considered to have no significant effect on the pressure drop.

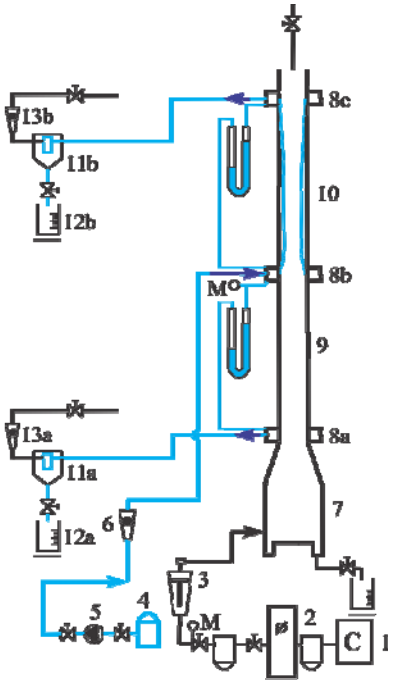

Fig. 2. Experimental set-up: a) line diagram: 1–compressor, 2–air dryer, 3–rotameter, 4–water tank, 5–pump, 6–rotameter, 7–air distributor, 8a,b,c–porous segment, 9–flow development section, 10–test section, 11a,b–gas–liquid separators,12a,b–measuring vessel.

Distillated water from a water tank (4) is circulated by a variable speed gear pump (5). The water flow rate is measured by a rotameter (6) with an accuracy of ±2%. After leaving the rotameter, the water flows into the test section (10) through a porous segment (8b) at the bottom of the test section. In the experiment, air from a compressor (1) passes first through a refrigerated air dryer (2) to remove the moisture and later through an oil filter to eliminate the oil content. The air flow rate was regulated by a pressure regulator and a valve and measured by means of a calibrated rotameter (3). The air velocity in the test section is calculated from the measured air flow rate, temperature and pressure. The flow rate of the air–water mixture is controlled by a valve and the removed air is measured by a rotameter (13b) installed after the gas–liquid separator (13b).

Air humidity and temperature at the inlet and outlet of the test section and the pressure difference along the test section are measured. Partial pressures are determined from the measured relative humidity at the inlet and the outlet of the test section, and Eq. (5) is used to calculate the Sherwood number. The liquid flow rate at which the entrained droplet was observed in the section after the upper porous segment indicates the critical liquid flow rate, M_{FC}, at which atomization of the liquid film occurs. Liquid film atomization is not observed in the experiment. The critical liquid film Reynolds number $\mathrm{Re}_{FC} = 4M_{FC}/\pi d\mu_L$, at which the liquid film atomization occurs, in terms of the gas Reynolds number is reported by [18].

IV. EXPERIMENTAL RESULTS

A. Adiabatic evaporation

The experimental results of adiabatic liquid film for vertical upward co-current annular flow are shown as the Sherwood number in terms of the gas Reynolds number. The variation of the average Sherwood number against the air Reynolds number (Re_G) in a range from 25000 to 70000, are shown in Fig. 3. Relative air humidity at the inlet of test section varied from 1% (using a silica gel dryer) to 14.5%.

Water flow rate was in the ranged from 1.6 dm^3/h to 4.6 dm^3/h. The average Sherwood number, defined as $\mathrm{Sh} = k_G RTD/D_{AB}$, in terms of the Reynolds number is obtained as

$$\mathrm{Sh} = 0.0526\,\mathrm{Re}^{0.66}\,\mathrm{Sc}^{0.33} \qquad (12)$$

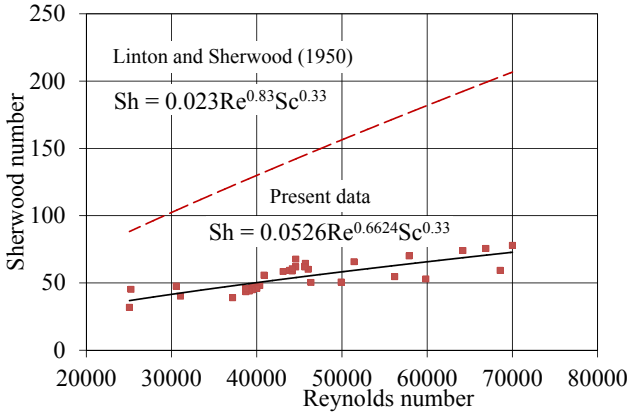

Fig. 3. The Sherwood number in terms of the Reynolds number.

Above correlation is compared to the Linton and Sherwood [19] correlation for turbulent mass transfer in a pipe flow. The correlation [19] gives 2.3 times larger Sherwood number at Re_G=25000 and 2.67 times at Re_G=70000 than that obtained in the present experiment, as Fig. 4 shows.

B. *Friction factor*

The Fanning friction factor against the gas Reynolds number is shown in Fig. 4. The Fig. 4 compares present experimental data and Eq. (7).

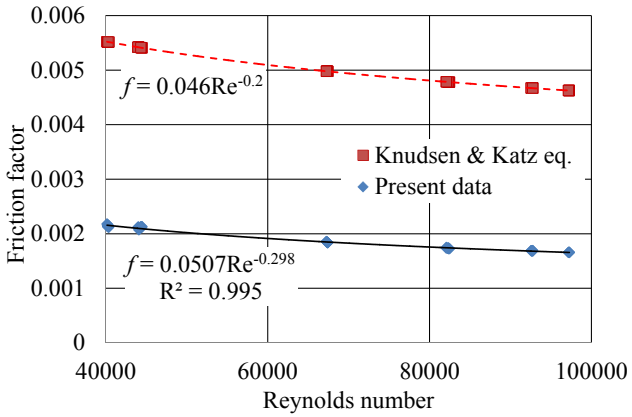

Fig. 4. The friction factor: present experimental data and Eq. (7).

The friction factors are determined for the water flow rates. The flow rate varied from 0.48×10^{-5} to 16.74×10^{-5} kg/s, and the corresponding liquid film Reynolds number varied from 0.37 to 13. The air flow rate ranged from 7.56×10^{-3} to 18.38×10^{-3} kg/s and the gas Reynolds number 43000 to 97000.

In this study, as the best fit for predicting the Fanning friction factor in air–water two-phase flow, power law is used

$$f = 0.0507\,\mathrm{Re}_G^{-0.298} \qquad (13)$$

In this experiment, the friction factor was less than that that predicted by Eq. (7). Evaporating thin liquid film, which flows parallel to the gas, influences pressure drop and reduces the friction factor. It also influenced the mass transfer coefficient. The mass transfer correlation based on the heat transfer analogy overpredicts the mass transfer coefficient, here expressed in dimensionless form as the Sherwood number. The height of the liquid layers is not measured in this experiment.

The dimensionless height of the liquid layer estimated using Eq. (9) is about 1 μm. The height of the liquid film was also predicted from the ratio f_i/f_S, given by Eq. (11), where f_i is calculated from the experimental data and f_S is estimated from Eq. (7). For these data, the height of the liquid films is about 27 μm.

V. CONCLUSION

Initial experimental work has been carried out to investigate evaporation of water in a vertical upward co-current annular flow under adiabatic conditions. The experimental results, as the Sherwood number in terms of the air Reynolds number are correlated by power law in terms of the air Reynolds numbers. The experimentally obtain data show much lower values than the correlation proposed by Linton and Sherwood [19]. The results from current study indicate that the evaporating thin liquid film reduces the friction factor. While a greater height of the liquid layer contribute to a rapid increase of the friction factor. Further experiments are needed for a better understanding adiabatic evaporation liquid film driven by a fast moving gas.

References

[1] S.S. Kutateladze and I.I. Gogonin, Heat transfer in film condensation of slowly moving vapour. Int. J. Heat Mass Transfer 22, 1979, pp. 1593–1599.

[2] S. Jayanti and G. F. Hewitt, Hydrodynamics and heat transfer of wavy thin film flow. Int. J. Heat Mass Transfer 40 (1), 1995, pp. 179–190.

[3] A. Miyara, Numerical analysis on flow dynamics and heat transfer of falling liquid films with interfacial waves. Heat Mass Transfer 35, 1999, pp. 298–306.

[4] E.O. Doro, Computational Modeling of Falling Liquid Film Free Surface Evaporation, PhD Thesis, Georgia Institute of Technology, 2012.

[5] J. Grünig, E. Lyagin, S. Horn, T. Skale and M. Kraume, Mass transfer characteristics of liquid films flowing down a vertical wire in a counter current gas flow. Chemical Engineering Science vol. 69, 2012, p. 329.

[6] P.L. Spedding and M.T. Jones, Heat and mass transfer in wetted-wall columns: I. The Chemical Engineering Journal, 37, 1988, p. 165.

[7] A.B. Erasmus and I. Nieuwoudt, Mass transfer in structured packing: A wetted-wall study. Industrial & Engineering Chemistry Research, 40, 2001, p. 2310.

[8] W.H. Henstock and T.J. Hanratty, Gas Absorption by a Liquid Layer Flowing on the Wall of a Pipe. AIChE Journal 25, 1979, p. 122.

[9] H. Hikita and K. Ishimi, A simplified method of estimating mass and heat transfer coefficients for turbulent gas streams in wetted-wall columns. Journal of Chemical Engineering of Japan, 20, 1987, p. 185.

[10] P.N. Yoshimura, T. Nosoko and T. Nagata, Enhancement of mass transfer into a falling laminar liquid film by twig-dimensional surface waves - Some experimental observations and modeling. Chemical Engineering Science, 51, 1996, p. 1231.

[11] C.D. Park and T. Nosoko, Three-Dimensional Wave Dynamics on a Falling Film and Associated Mass Transfer. AIChE Journal, 49, 2003, p. 2715.

[12] C.H.E. Nielsen, S. Kiil, H.W. Thomsen and K. Dam-Johansen, Mass transfer in wetted-wall columns: Correlations at high Reynolds numbers. Chemical Engineering Science, 53, 1998, pp. 495–503.

[13] F. Garcia, J.M. Garcia, R. Garcia, D.D. Joseph, Friction factor improved correlations for laminar and turbulent gas–liquid flow in horizontal pipelines, Int. J. Multiphase Flow, 33, 2007, pp. 1320–1336.

[14] R.E. Treybal, Mass Transfer Operations, 3rd ed. McGraw-Hill, New York, 1980.

[15] J. G. Knudsen and D. L. Katz, Fluid Dynamics and Heat Transfer, McGraw-Hill, New York, 1958, pp. 89, 173.

[16] W. H. Henstock and T. J. Hanratty, The interfacial drag and the height of the wall layer in annular flows. AIChE Jl 22, 1976, pp. 990–1000.

[17] J.C. Asali, T.J. Hanratty and P. Andreussi, Interfacial drag and film height for vertical annular flow. AICh Jl 31, 1985, pp. 895–902.

[18] Š. Šikalo, N. Delalić and E.N. Ganić, Hydrodynamics and heat transfer investigation of air–water dispersed flow. Exp. Therm. Fluid Sci., 25, 2002, pp. 511–521.

[19] W.H.J. Linton and T.K. Sherwood, Mass transfer from solid shapes to water in streamline and turbulent flow. Chem. Eng. Progr., 46, 1950, pp. 258–264.